Monthly Notices
of the
ROYAL ASTRONOMICAL SOCIETY

Mon. Not. R. Astron. Soc. **424,** 65–79 (2012) doi:10.1111/j.1365-2966.2012.21152.x

The influence of stellar dynamical ejections and collisions on the relation between the maximum stellar and star cluster mass

Seungkyung Oh★† and Pavel Kroupa

Argelander-Institut für Astronomie, Auf dem Hügel 71, 53121 Bonn, Germany

Accepted 2012 April 20. Received 2012 April 2; in original form 2011 June 22

ABSTRACT

We perform the largest currently available set of direct *N*-body calculations of young star cluster models to study the dynamical influence, especially through the ejections of the most massive star in the cluster, on the current relation between the maximum stellar mass and the star cluster mass. We vary several initial parameters such as the initial half-mass radius of the cluster, the initial binary fraction and the degree of initial mass segregation. Two different pairing methods are used to construct massive binaries for more realistic initial conditions of massive binaries. We find that lower mass clusters ($\leq 10^{2.5}\,\mathrm{M}_\odot$) do not shoot out their heaviest star. In the case of massive clusters ($\geq 1000\,\mathrm{M}_\odot$), no most massive star escapes the cluster within 3 Myr regardless of the initial conditions if clusters have initial half-mass radii, $r_{0.5}$, ≥ 0.8 pc. However, a few of the initially smaller sized clusters ($r_{0.5} = 0.3$ pc), which have a higher density, eject their most massive star within 3 Myr. If clusters form with a compact size and their massive stars are born in a binary system with a mass ratio biased towards unity, the probability that the mass of the most massive star in the cluster changes due to the ejection of the initially most massive star can be as large as 20 per cent. Stellar collisions increase the maximum stellar mass in a large number of clusters when clusters are relatively dense ($M_{\rm ecl} \geq 10^3\,\mathrm{M}_\odot$ and $r_{0.5} = 0.3$ pc) and binary rich. Overall, we conclude that dynamical effects hardly influence the observational maximum stellar mass–cluster mass relation.

Key words: methods: numerical – stars: kinematics and dynamics – stars: massive – open clusters and associations: general – galaxies: star clusters: general.

1 INTRODUCTION

Weidner, Kroupa & Bonnell (2010) compiled from the literature observational data of 100 young star clusters, whose masses lie between ≈10 and $2 \times 10^5\,\mathrm{M}_\odot$ and whose ages are younger than 4 Myr. They showed that observed young star clusters exhibit a well-defined correlation between the maximum stellar mass in the cluster, $m_{\rm max}$, and the mass in stars, $M_{\rm ecl}$, of the cluster. An upper age limit of 4 Myr was chosen in order to minimize any evolutionary effects on the sample. The examples of evolutionary effects discussed in their paper are as follows. First, mass-loss of massive stars due to stellar evolution may influence the cluster mass. Secondly, gas expulsion leads the cluster to lose a significant amount of its stars (i.e. cluster mass) by weakening of the gravitational potential when the residual gas is expelled from the cluster. However, these effects unlikely affect $M_{\rm ecl}$ owing to the young ages of the clusters in the Weidner et al. (2010) sample. The authors corrected $m_{\rm max}$ for stellar evolution in the case of O-type stars (note that later than O-type stars would not have evolved much at this young age), so that the $m_{\rm max}$ values provided in their paper can be considered as initial values. One process they did not take account of is the dynamical ejection of the most massive star from the cluster. The authors commented that it is highly unlikely to happen. But this has not been studied thoroughly so far. Thus, it is our aim in this study to investigate how often a young star cluster ejects its most massive member.

This observed correlation fits a semi-analytical model well (Weidner & Kroupa 2004, 2006; Weidner et al. 2010) which is deduced from there being exactly one most massive star in the cluster,

$$1 = \int_{m_{\rm max}}^{m_{\rm max*}} \xi(m)\,\mathrm{d}m, \tag{1}$$

subject to the normalization

$$M_{\rm ecl} = \int_{m_{\rm low}}^{m_{\rm max}} m\xi(m)\,\mathrm{d}m, \tag{2}$$

where $m_{\rm max*} \approx 150$–$300\,\mathrm{M}_\odot$ is the fundamental upper limit of stellar masses (Weidner & Kroupa 2004, 2006; Figer 2005; Oey

★Member of the International Max Planck Research School (IMPRS) for Astronomy and Astrophysics at the Universities of Bonn and Cologne.
†E-mail: skoh@astro.uni-bonn.de

& Clarke 2005; Crowther et al. 2010), $m_{\rm low} = 0.08\,{\rm M}_\odot$ is the hydrogen burning mass limit (brown dwarfs contribute negligibly to the cluster mass; Thies & Kroupa 2007) and $\xi(m)$ is the stellar initial mass function (IMF). A pure size-of-sample effect as expected from random sampling has been excluded as an origin of the observed correlation. Details of previous studies on the $m_{\rm max}-M_{\rm ecl}$ relation can be found in Weidner & Kroupa (2004, 2006), Weidner et al. (2010) and references therein. Note that Maschberger & Clarke (2008) argued that at least for the low-N clusters (i.e. low-mass clusters) observed maximum stellar masses do not much deviate from random drawing. This is basically true but leads the reader to the misinterpretation that a physical origin of the most massive star in these clusters is ruled out. But Weidner et al. (2010) show that in the mass regime considered by Maschberger & Clarke (2008) a physical $m_{\rm max}$ and a stochastic $m_{\rm max}$ cannot be distinguished from each other. The observed clusters from Weidner et al. (2010) and their semi-analytical relation are reproduced in Fig. 1. Interestingly, a similar relation appears in numerical simulations of star cluster formation as well. Smoothed particle hydrodynamics numerical simulations of massive star formation driven by competitive accretion (Bonnell, Vine & Bate 2004) showed that the most massive star in the forming cluster grows following the relation $m_{\rm max}(t) \propto M_{\rm ecl}(t)^{2/3}$ with time, t, which is a best fit to their simulation data. This fit agrees with the semi-analytical $m_{\rm max}-M_{\rm ecl}$ relation very well for clusters with $M_{\rm ecl} \lesssim 10^3\,{\rm M}_\odot$. Furthermore, a fragmentation-induced starvation scenario studied with radiation-hydrodynamical simulations of massive star formation using the adaptive-mesh code FLASH (Peters et al. 2010) also reproduced the relation found by Bonnell et al. (2004). Data from the numerical simulations of star cluster formation including the two studies mentioned above are also plotted in Fig. 1. The simulation data are in good agreement with the observed data.

Although most of the clusters follow the relation well, there is a spread of $m_{\rm max}$ values at a given cluster mass. Is this spread due to stochastic effects that occur during the formation of a cluster, or does it mask a true physical functional dependence of $m_{\rm max}$ on $M_{\rm ecl}$? Dynamical processes can exert an influence on the relation during the early evolution of the cluster. Stars can be dynamically ejected through energetic few body interactions. The lightest star among the interacting stars generally obtains the highest velocity and it is unlikely that the most massive star is ejected. Several theoretical studies, nevertheless, have shown that massive stars can be dynamically ejected under certain circumstances such as from a small group of massive stars lacking low-mass stars (Clarke & Pringle 1992; Gvaramadze, Gualandris & Portegies Zwart 2009; Fujii & Portegies Zwart 2011; Gvaramadze & Gualandris 2011), through binary–single (Hills & Fullerton 1980) and binary–binary interactions (Leonard & Duncan 1990). The high efficiency of dynamical ejections from dense stellar systems can indeed explain the difference between the observed and expected number of OB-type stars in the Orion nebula cluster (ONC; Pflamm-Altenburg & Kroupa 2006). Furthermore, dense and massive R136-type clusters are efficient in expelling massive stars (Banerjee, Kroupa & Oh 2012). Thus it may be possible that the heaviest star in a cluster be dynamically ejected from the cluster.

In this contribution we assume that there exists an exact function, $m_{\rm max} = {\rm fn}({\rm M}_{\rm ecl})$, and we study the ejection of the heaviest star in a cluster using direct N-body integration to investigate the effect on the $m_{\rm max}-M_{\rm ecl}$ relation. Details of the initial conditions of the cluster models and of the calculations are described in Section 2 and then results are shown in Section 3. The discussion and the conclusions follow in Sections 4 and 5.

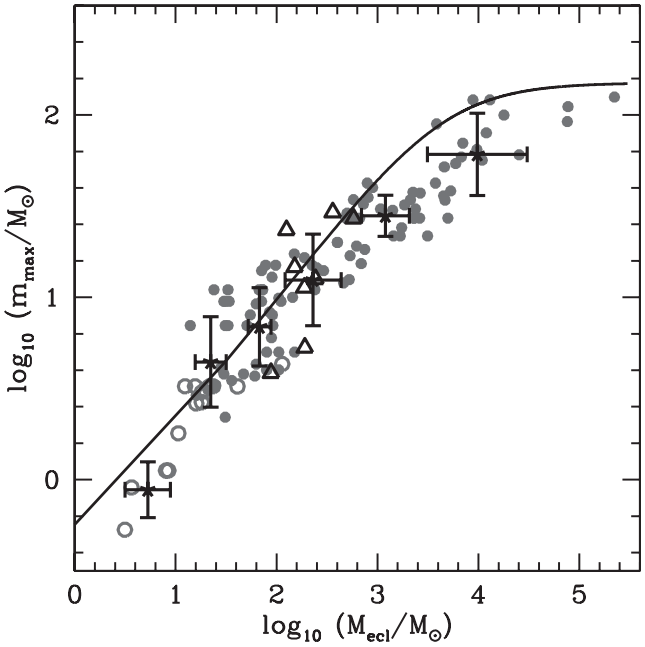

Figure 1. Mass of the most massive star versus cluster mass from observational data in Weidner et al. (2010). Each grey filled circle is a star cluster from their table B1. The black solid line is the semi-analytical $m_{\rm max}-M_{\rm ecl}$ relation from equations (1) and (2) assuming an upper limit of the stellar mass of $150\,{\rm M}_\odot$ (Weidner & Kroupa 2004, 2006). The open circles are the mass of the most massive member in the group versus the total group mass in 14 young stellar groups in Taurus, Lupus3, ChaI and IC348 (Kirk & Myers 2011). These young (low-mass) stellar groups also follow the $m_{\rm max}-M_{\rm ecl}$ relation well. The black points and error bars represent the average and standard deviation of $\log_{10}M_{\rm ecl}$ and $\log_{10}m_{\rm max}$ in each bin each of which contains 22 clusters for the upper five bins and four clusters for the lowest cluster mass bin. Data from several numerical simulations of star formation (Bonnell et al. 2004; Bate 2009, 2012; Smith, Longmore & Bonnell 2009; Peters et al. 2010) are included in the figure as open triangles.

2 MODELS

We perform a large set of direct N-body calculations of young star clusters using NBODY6 (Aarseth 1999) with various initial conditions. Cluster masses range from 10 to $10^{3.5}\,{\rm M}_\odot$ with an interval of 0.5 on the logarithmic scale and each mass is initialized with two different half-mass radii, $r_{0.5} = 0.3$ and 0.8 pc. To study the effect of binaries, we adopt two extreme binary fractions which are 0 (all stars are single) and 1 (all stars are in binary systems). The initial binary population used in this study is described in Section 2.1. Single star clusters (all stars are single) are chosen for comparison purpose only since most stars in actuality form in a binary system (Goodwin & Kroupa 2005).

For each cluster mass the number of stars, $N_{\rm star}$, is assigned by dividing the cluster mass by the average stellar mass of the cluster

$$N_{\rm star} = \frac{M_{\rm ecl}}{\langle m \rangle}, \tag{3}$$

where the average stellar mass of the cluster, $\langle m \rangle$, is

$$\langle m \rangle = \frac{\int_{m_{\rm low}}^{m_{\rm max}} m\xi(m)\,{\rm d}m}{\int_{m_{\rm low}}^{m_{\rm max}} \xi(m)\,{\rm d}m}.$$

We adopt the canonical two-part power-law IMF (Kroupa 2001; Kroupa et al. 2012),

$$\xi(m) \propto m^{-\alpha_i}, \tag{4}$$

where

$$\alpha_1 = 1.3, \quad 0.08 \leq m/{\rm M}_\odot < 0.50,$$
$$\alpha_2 = 2.3, \quad 0.50 \leq m/{\rm M}_\odot \leq m_{\rm max}.$$

We use $m_{\rm max,WK} \equiv m_{\rm max}$, which is calculated using the semi-analytical relation (equations 1 and 2) assuming the fundamental upper limit of stellar masses to be $m_{\rm max*} = 150\,{\rm M}_\odot$. The solid line in Fig. 1 represents $m_{\rm max,WK}$.

Individual masses of all stars but one (i.e. $N_{\rm star} - 1$ stars) in each cluster are randomly drawn from the IMF (equation 4) with a stellar mass range from $0.08\,{\rm M}_\odot$ to $m_{\rm max,WK}$. To simplify the analysis, one $m_{\rm max,WK}$ star is added so that every cluster has at least one star with a mass of $m_{\rm max,WK}$.[1] This procedure removes the stochastic effects on the initial $m_{\rm max}$. This choice, however, gives a bump at the most massive mass bin in the IMF of the cluster, which is especially significant in small-N (i.e. low-mass) clusters. As the dynamical ejection of massive stars occurs by close encounters between massive stars (Leonard & Duncan 1990; Clarke & Pringle 1992), our enforcement of having a $m_{\rm max,WK}$ star may enhance the ejections at a given $M_{\rm ecl}$ by overpopulating massive stars. We find that this choice would not change our conclusion (see further discussion in Section 4).

Positions and velocities of stars in the cluster are generated according to the Plummer model (Aarseth, Hénon & Wielen 1974) which is the simplest stationary solution of the collisionless Boltzmann equation (Heggie & Hut 2003; Kroupa 2008) and is an excellent description of the nearest star cluster, the Hyades (Röser et al. 2011). To study the effect of initial mass segregation, half of our cluster models are initially mass segregated. The method for constructing initially mass-segregated clusters in which positions and velocities are dependent on stellar masses is described in Section 2.2. For unsegregated clusters, positions and velocities are assigned to stars independently of their masses.

Dynamical time-scales such as the crossing time and the median two-body relaxation time are important tools to estimate the dynamical evolution of stellar systems. The initial crossing time is

$$t_{\rm cr} = \frac{2r_{0.5}}{\sigma}, \tag{5}$$

where σ is initial velocity dispersion, $\sigma = \sqrt{GM_{\rm ecl}/r_{\rm grav}}$, $r_{\rm grav} \approx 2.6r_{0.5}$ is the gravitational radius (Binney & Tremaine 1987; Kroupa 2008). The relaxation time is

$$t_{\rm rel} = 0.1\frac{N_{\rm star}}{\ln N_{\rm star}} t_{\rm cr}. \tag{6}$$

Initial conditions of all cluster models are listed in Table 1. Table 2 shows the physical properties of the six different mass clusters. All clusters are evolved up to 5 Myr. And stellar evolution is taken into account using the stellar evolution library (Hurley, Pols & Tout 2000) in the NBODY6 code. We carry out 100 computations for each set of initial conditions. In total 7200 models are thus calculated with a standard desktop PC. In addition, we perform 10 calculations for clusters with $M_{\rm ecl} = 10^4\,{\rm M}_\odot$ and with the same initial conditions as MS3OP in Table 1. We compute only the most energetic cluster model (MS3OP) in our library for $M_{\rm ecl} = 10^4\,{\rm M}_\odot$ because of the high computational cost for massive clusters. This is the largest currently existing systematically generated library of young star cluster models.

[1] This procedure would not be required if optimal sampling of stellar masses from the IMF (Kroupa et al. 2012) were used instead of random sampling. Optimal sampling was not available though at the time the present library of clusters was computed.

Table 1. The initial conditions of cluster models. Model name is in the first column. Column 2 indicates the initial mass segregation, N standing for an initially unsegregated cluster while Y signifying an initially segregated cluster. Columns 3 and 4 present the initial half-mass radius of the cluster, $r_{0.5}$, and the initial binary fraction, $f_{\rm bin,i}$, respectively. OP and RP in the $f_{\rm bin,i}$ column represent the pairing method for the massive binaries: ordered pairing and random pairing, respectively. The description of the pairing methods can be found in Section 2.1.

Model	Mass segregation	$r_{0.5}$ (pc)	$f_{\rm bin,i}$
NMS3S	N	0.3	0
NMS3RP	N	0.3	1 (RP)
NMS3OP	N	0.3	1 (OP)
NMS8S	N	0.8	0
NMS8RP	N	0.8	1 (RP)
NMS8OP	N	0.8	1 (OP)
MS3S	Y	0.3	0
MS3RP	Y	0.3	1 (RP)
MS3OP	Y	0.3	1 (OP)
MS8S	Y	0.8	0
MS8RP	Y	0.8	1 (RP)
MS8OP	Y	0.8	1 (OP)

2.1 Primordial binaries

To set up the primordial binaries we require their initial orbital parameters such as periods, eccentricities and mass ratios. The initial period distribution adopted in this study is equation 8 in Kroupa (1995b),

$$f_{\rm P} = 2.5\frac{\log_{10} P - 1}{45 + (\log_{10} P - 1)^2}, \tag{7}$$

where period, P, is in days. With this distribution function, minimum and maximum log periods, $\log_{10}P_{\rm min}$ and $\log_{10}P_{\rm max}$, are 1 and 8.43, respectively. This function shows a flat distribution at long periods and is in good agreement with the period distribution of low-density young stellar aggregates such as Taurus–Auriga (Kroupa & Petr-Gotzens 2011; Marks, Kroupa & Oh 2011). The initial eccentricity distribution follows the thermal distribution, $f(e) = 2e$ (Kroupa 2008). Pre-main-sequence eigenevolution (Kroupa 1995b) is not included in our calculations as our emphasis is on the massive stars.

The initial mass ratios of low-mass stars such as G-, K- and M-dwarf binaries can be well described with random pairing (RP; Kroupa 1995a, 2008). Observational studies of OB-type binaries, however, show that they tend to have similar mass companions (García & Mermilliod 2001; Sana et al. 2008; Sana, Gosset & Evans 2009). Sana & Evans (2011) show that the mass-ratio distribution of O star binaries seems uniform in the range $0.2 \leq m_2/m_1 \leq 1.0$, m_1 being the primary and m_2 the secondary mass. In any case the mass ratios of massive binaries are high compared to low-mass stars. RP cannot produce the observed mass-ratio distribution of massive binaries since it typically leads to massive stars being paired with low-mass stars which are the majority in the cluster. Thus, RP over the whole stellar mass range for OB star primaries is ruled out by the observation. A different pairing method for masses of binary components is needed to create massive binaries.

In this study we introduce a simple method to generate massive binaries having mass ratios biased towards unity. First, all stellar masses are randomly drawn from the IMF and then, stars more massive than $5\,{\rm M}_\odot$ are sorted with decreasing mass and the others are retained in random order. We pair stellar masses in order

Table 2. Characteristics of clusters with different sizes and masses. Cluster mass, $M_{\rm ecl}$, number of stars in a cluster, $N_{\rm star}$, initial mass of the most massive star in the cluster, $m_{\rm max,i}$ (from equations 1 and 2) and the tidal radius, $r_{\rm tid}$, are presented in columns 1–4. The $r_{\rm tid}$ is obtained from $r_{\rm tid} = R_{\rm GC}(M_{\rm ecl}/(3M_{\rm gal}))^{1/3}$ by assuming $M_{\rm gal}$, the Galactic enclosed mass within the Galactocentric distance ($R_{\rm GC}$) of 8.5 kpc, to be $5 \times 10^{10}\,{\rm M}_\odot$. The initial crossing, $t_{\rm cr}$, and the initial relaxation time, $t_{\rm rel}$, for two different cluster sizes, $r_{0.5} = 0.3$ and 0.8 pc, are given in columns 5–8. Each cluster model in Table 1 contains all six different mass clusters in this table. In total thus 72 different initial cluster configurations are used in this study, whereby 100 random realizations of each configuration are computed with Aarseth's NBODY6. The last model ($M_{\rm ecl} = 10^4\,{\rm M}_\odot$) is only computed 10 times and for the MS3OP configuration.

$M_{\rm ecl}$ (M$_\odot$)	$N_{\rm star}$	$m_{\rm max,i}$ (M$_\odot$)	$r_{\rm tid}$ (pc)	$t_{\rm cr}$ (Myr)		$t_{\rm rel}$ (Myr)	
				($r_{0.5} = 0.3$ pc	0.8 pc	0.3 pc	0.8 pc)
$10^{1.0}$	28	2.1	3.5	2.56	11.13	2.14	9.35
$10^{1.5}$	76	4.5	5.1	1.44	6.26	2.52	10.98
$10^{2.0}$	214	9.7	7.4	0.81	3.52	3.22	14.03
$10^{2.5}$	618	21.2	10.9	0.45	1.98	4.37	19.03
$10^{3.0}$	1836	43.9	16.0	0.26	1.11	6.24	27.19
$10^{3.5}$	5584	79.2	23.5	0.14	0.63	9.30	40.50
$10^{4.0}$	17298	114.7	34.5	0.08	–	14.32	–

so that a massive star has the next massive one as a companion, while stars less massive than 5 M$_\odot$ have a companion which is randomly distributed. Thus, binaries with primary masses more massive than 5 M$_\odot$ have mass ratios biased towards unity. We call this method 'ordered pairing' (OP). Note that star clusters with masses $\lesssim$100 M$_\odot$ contain no stars more massive than 5 M$_\odot$ in this paper; thus, OP clusters with $M_{\rm ecl} \leq 10^{1.5}\,{\rm M}_\odot$ are the same as RP clusters. For a deep discussion on pairing methods for binaries, see Kouwenhoven et al. (2009) and Weidner, Kroupa & Maschberger (2009) who study several pairing mechanisms.

2.2 Primordial mass segregation

Many young star clusters exhibit evidence for mass segregation (Gouliermis et al. 2004; Chen, de Grijs & Zhao 2007). It has been under debate whether the observed mass segregation of young star clusters is the outcome of the star formation processes or of dynamical evolution of the clusters, since a certain time is needed for it to occur dynamically. Some observed clusters seem too young for mass segregation to have occurred. The dynamical mass segregation time-scale is

$$t_{\rm ms} \approx \frac{\langle m \rangle}{m_{\rm massive}} t_{\rm rel}, \tag{8}$$

where $m_{\rm massive}$ is the mass of the massive star. For some clusters, $t_{\rm ms}$ could be shorter than or comparable to their age (e.g. the Orion nebula cluster which has $t_{\rm ms}$ of about 0.1 Myr; Kroupa 2002). Thus, it is difficult to determine whether an observed mass segregation is primordial or the result of dynamical evolution. Studying the influence of primordial mass segregation on the early dynamical evolution of clusters would give a hint for an answer to this problem. However, it is beyond the scope of this paper as a deeper study on individual clusters is required to do that.

It is expected that initially mass-segregated clusters ought to be more efficient in ejecting massive stars, thus allowing the distribution of massive stars to be used as a constraint on the issue of initial mass segregation (Clarke & Pringle 1992; Gvaramadze & Bomans 2008; Gvaramadze et al. 2011). In order to create mass-segregated clusters we use the method introduced in Baumgardt, de Marchi & Kroupa (2008). Details of setting up the segregated cluster are described in their appendix. With this method, the heaviest star is most bound to the cluster and is located in the core of the cluster. And the cluster is initially in virial equilibrium and follows the Plummer density profile. Although one can vary the degree of mass segregation with this method, for simplicity, mass-segregated model clusters in this study are fully segregated. Thus, the segregated clusters have a core of massive stars in the centre of the cluster at the beginning of cluster evolution.

We stress that such *N*-body models of initially fully mass-segregated clusters with a 100 per cent binary fraction and a mass ratio near unity for the massive binaries have never been attempted before.

2.3 The *N*-body code

NBODY6 is a fully collisional *N*-body code which calculates the force on a particle from other particles with direct summation. It uses the Hermite scheme for integrating the orbits of stars. The code adapts individual time steps depending on the local environment and the Ahmad–Cohen neighbour scheme (Ahmad & Cohen 1973) for calculation efficiency. For treating close encounters, Kustaanheimo–Stiefel two-body regularization and chain regularization for higher order multiple systems are used.

Stellar evolution is implemented in the code using fitting functions with the Single Star Evolution package (Hurley et al. 2000) and the Binary Star Evolution package (Hurley, Tout & Pols 2002), which allows a collision between two components of a binary. Details of stellar evolution in NBODY6 can be found in Hurley (2008). Since we activate stellar evolution in the code, a star has a radius instead of being a point mass particle and may collide with other single stars or its companion in a binary system by close encounters and/or binary hardening. When they merge, a mass of one star is replaced by the sum of the colliding stars and the other star is replaced by a massless particle with a large distance so that it is removed from the calculation as a massless escaper (Aarseth 2003). A metallicity of $Z = 0.02$ (solar) is adopted in all our calculations.

3 RESULTS

Clusters keep losing their mass due to stars escaping from them via the two-body relaxation process or through dynamical ejections

besides stellar evolution, and so we only count stars found inside the tidal radius as cluster members. A cluster mass does not change much (at most ≈3 per cent on average by 3 Myr) within the first few Myr. Therefore, the change of the $m_{\rm max}-M_{\rm ecl}$ relation within the first few Myr is mainly caused by the change of $m_{\rm max}$. There are three ways to change the maximum stellar mass as a cluster evolves. First, stellar evolution changes the mass of the heaviest star in the cluster. Stars lose their mass with time via stellar winds. The mass-loss rate is dependent on the stellar mass. The more massive a star the larger is its mass-loss rate. In the case of the most massive cluster in our model ($M_{\rm ecl} = 10^{3.5}\,{\rm M}_\odot$), its heaviest star with an initial mass of ≈80 $\rm M_\odot$ loses mass to become an ≈64 $\rm M_\odot$ star at 3 Myr. On the other hand, for clusters with $M_{\rm ecl} \leq 10^3\,{\rm M}_\odot$, $m_{\rm max}$ remains almost the same as the initial value since the heaviest stars in such clusters do not evolve much in a few Myr. Secondly, stars can physically collide. If two stars collide and become a more massive star than the initially heaviest star, or if the initially heaviest star collides with another star, then the new heaviest star will lie off the initial relation. Massive stars generally move into the cluster centre which has a high stellar density. Thus, a massive star may collide with another massive star in the cluster centre. Lastly, dynamical ejection of the initially heaviest star in the cluster also changes $m_{\rm max}$ by replacing it with the initially second massive star in the cluster.

Stellar evolution and dynamical ejection lead to the cluster having a smaller maximum stellar mass, while stellar collisions increase the maximum stellar mass in the cluster. In our models all three of these effects occur. However, here we concentrate only on stellar collisions and ejections as the initial masses of the heaviest stars are set to be equal for the same cluster mass. Thus, stellar evolution does not produce the $m_{\rm max}$ spread at the same cluster mass. And we are particularly interested in how often the heaviest star is ejected from the clusters.

Using direct N-body calculations, we study the dynamical effect on the $m_{\rm max}-M_{\rm ecl}$ relation with various initial conditions of the clusters (Tables 1 and 2). Although the clusters are evolved up to 5 Myr, we only use the results up to 3 Myr since stellar evolution begins to play a dominant role in changing the value of $m_{\rm max}$ of the $10^{3.5}\,{\rm M}_\odot$ cluster at around 3.5 Myr. The initially most massive star of the $10^{3.5}\,{\rm M}_\odot$ cluster becomes a black hole after 4 Myr. Furthermore, most of the observed clusters used in the study of the $m_{\rm max}-M_{\rm ecl}$ relation (Weidner et al. 2010) are younger than 3 Myr.

For clarification, we refer to the heaviest star in the cluster at 0 Myr as $S_{\rm MAXI}$ and to the mass of the most massive star in the cluster at a given snapshot as $m_{\rm max}$.

3.1 Dynamical ejection of $S_{\rm MAXI}$

Stars can be ejected from a cluster via close encounters between a hard binary and a single star/binary. During the encounter, the hard binary gives its binding energy to the interacting star/stars in the form of kinetic energy and it hardens. The star that gained kinetic energy may be ejected from the cluster. Generally, the lightest one among the interacting stars attains the highest velocity after the interaction. Thus, the dynamical ejection of massive stars preferably occurs from interactions between massive stars. Leonard & Duncan (1990) showed that binary–binary interactions are the most efficient way for producing massive runaways.

We consider $S_{\rm MAXI}$ to be dynamically ejected if the star is further away from the cluster centre than the tidal radius of the cluster. The number of clusters which eject their $S_{\rm MAXI}$, $N_{\rm resc}$, is listed in Table 3 for all cluster models.

In the following subsections, results on the dynamical ejection of $S_{\rm MAXI}$ are discussed separately for models with different initial half-mass radii.

3.1.1 *The $r_{0.5} = 0.8$ pc models*

In Table 3, there are two clusters with $r_{0.5} = 0.8$ pc whose $S_{\rm MAXI}$ is located further than the tidal radius of the cluster at 3 Myr. The most massive star of one not initially mass-segregated $10\,{\rm M}_\odot$ cluster was, in fact, located outside of the tidal radius of the cluster, which is ≈3.5 pc, at 0 Myr. Therefore, this case is not due to dynamical ejection. Thus, only one out of 3600 model clusters with $r_{0.5} = 0.8$ pc eject their $S_{\rm MAXI}$ within 3 Myr.

Fig. 2 shows the $m_{\rm max}-M_{\rm ecl}$ relation of the binary-rich clusters with $r_{0.5} = 0.8$ pc and massive binaries paired by the OP method (models NMS8OP and MS8OP) at different ages of the clusters. Even though this set of initial conditions is the most dynamic case of the cluster models with $r_{0.5} = 0.8$ pc, only one cluster, with a mass of $10^{3.5}\,{\rm M}_\odot$, ejects its $S_{\rm MAXI}$ (Table 3). But the initially second heaviest star of the cluster, which becomes the most massive one in the cluster after ejection of $S_{\rm MAXI}$, has a similar mass to the mass of $S_{\rm MAXI}$. Therefore, the effect of the ejection on the $m_{\rm max}-M_{\rm ecl}$ relation is negligible in this case.

It is unlikely that the $m_{\rm max}-M_{\rm ecl}$ relation is affected by the dynamical ejection of $S_{\rm MAXI}$ for clusters of this size. But it is worthy to note that at 3 Myr a few OP clusters show their $S_{\rm MAXI}$ moving faster than the escape velocity, $v_{\rm esc}(r) = \sqrt{2|\Phi(r)|}$, where $\Phi(r)$ is the gravitational potential at a distance r from the cluster centre, although these clusters barely eject their $S_{\rm MAXI}$ (Table 3).

3.1.2 *The $r_{0.5} = 0.3$ pc models*

Fig. 3 shows the $m_{\rm max}-M_{\rm ecl}$ relation for the binary-rich cluster models with $r_{0.5} = 0.3$ pc. Despite the smaller size of the clusters, none of the single star clusters (NMS3S and MS3S) eject their most massive star (Table 3). Only two massive clusters with $M_{\rm ecl} = 10^{3.5}\,{\rm M}_\odot$ eject their $S_{\rm MAXI}$ when the massive binaries are randomly paired (NMS3RP and MS3RP in Table 3). However, binaries help the most massive star to attain a higher velocity compared to the single star clusters. The number of clusters for which the heaviest star has a speed exceeding the escape velocity is larger when the stars are initially in a binary system (Table 3).

Clusters with $M_{\rm ecl} \leq 10^{2.5}\,{\rm M}_\odot$ hardly eject their most massive star even though the clusters form in energetic initial conditions such as being binary rich and mass segregated. Among all clusters with $M_{\rm ecl} \leq 10^{2.5}\,{\rm M}_\odot$, only one out of 100 clusters with $M_{\rm ecl} = 10^2\,{\rm M}_\odot$ and two out of 100 clusters with $M_{\rm ecl} = 10^{2.5}\,{\rm M}_\odot$ eject their $S_{\rm MAXI}$ (Table 3). However, at 3 Myr there are a few clusters whose $S_{\rm MAXI}$ is inside the tidal radius but has a velocity higher than the escape velocity so that it may leave the cluster later.

For clusters with $M_{\rm ecl} \geq 10^3\,{\rm M}_\odot$, 15–40 per cent of the most energetic models (MS3OP) have $S_{\rm MAXI}$ moving faster than the escape velocity and 2–20 per cent of the clusters have ejected their $S_{\rm MAXI}$ at 3 Myr. When the clusters are initially mass segregated, slightly more clusters eject $S_{\rm MAXI}$.

Fig. 4 shows the ejection frequency of $S_{\rm MAXI}$ as a function of the cluster mass for the MS3OP models. We only plot these models since the other models barely eject their initially most massive star (see Table 3 for all models). The ejection probability of the $S_{\rm MAXI}$ star increases with the cluster mass as the stellar density increases. About 8 (20) per cent of $10^{3.5}$ (10^4) $\rm M_\odot$ clusters eject their $S_{\rm MAXI}$ within 3 Myr (squares in Fig. 4). Some massive clusters which eject

Table 3. Results at 3 Myr. $M_{\rm ecl}$ is a cluster mass in $M_\odot$ (per $M_{\rm ecl}$ value there are 100 clusters, but 10 clusters for $10^4\,M_\odot$). $N_{\rm resc}$ is the number of clusters whose $S_{\rm MAXI}$ is located beyond the tidal radius of the cluster. $N_{\rm vesc}$ is the number of clusters whose $S_{\rm MAXI}$ has a velocity larger than the escape velocity. $N_{\rm vesc10}$ is the number of clusters whose $S_{\rm MAXI}$ is located further than 10 pc from the cluster centre and has a velocity larger than the escape velocity. $N_{\rm c}$ is the number of clusters whose $m_{\rm max}$ changes due to stellar collisions. Numbers in brackets indicate the collision products that do not involve $S_{\rm MAXI}$. For example, in the case of clusters with $M_{\rm ecl} = 10^{3.5}\,M_\odot$ from the NMS3RP model, one out of 100 clusters lose its $S_{\rm MAXI}$ by dynamical ejection, $S_{\rm MAXI}$ of six clusters have a velocity greater than the escape velocity of the cluster, and for two clusters out of these six clusters the star is located beyond 10 pc from the cluster centre. Stellar collisions which change the $m_{\rm max}$ have occurred in 51 clusters; for 11 clusters out of these 51 the collisions do not involve $S_{\rm MAXI}$.

$M_{\rm ecl}\,(M_\odot)$	$N_{\rm resc}$	$N_{\rm vesc}$	$N_{\rm vesc10}$	$N_{\rm c}$	$N_{\rm resc}$	$N_{\rm vesc}$	$N_{\rm vesc10}$	$N_{\rm c}$
	Unsegregated cluster model				Mass-segregated cluster model			
	NMS3S				MS3S			
10	0	0	0	0	0	0	0	0
$10^{1.5}$	0	0	0	0	0	0	0	0
10^{2}	0	0	0	0	0	0	0	0
$10^{2.5}$	0	0	0	0	0	1	0	2
10^{3}	0	0	0	6 (1)	0	2	0	8
$10^{3.5}$	0	6	1	36 (8)	0	5	1	36 (4)
	NMS3RP				MS3RP			
10	0	1	0	0	0	2	0	0
$10^{1.5}$	0	0	0	0	0	2	0	1 (1)
10^{2}	0	1	0	1	0	0	0	2
$10^{2.5}$	0	0	0	8 (2)	0	4	0	9 (1)
10^{3}	0	2	0	17 (3)	1	4	1	23 (1)
$10^{3.5}$	1	6	2	51 (11)	1	7	4	46 (4)
	NMS3OP				MS3OP			
10	0	1	0	0	0	2	0	0
$10^{1.5}$	0	4	0	2	0	2	0	0
10^{2}	0	5	0	1	1	5	1	1
$10^{2.5}$	0	14	0	5 (1)	2	23	2	4
10^{3}	1	15	2	23 (4)	2	15	3	17 (3)
$10^{3.5}$	6	15	7	60 (23)	8	24	12	56 (14)
10^{4}					2	4	4	9 (4)
	NMS8S				MS8S			
10	1	0	0	0	0	0	0	0
$10^{1.5}$	0	0	0	0	0	0	0	0
10^{2}	0	0	0	0	0	0	0	0
$10^{2.5}$	0	0	0	0	0	0	0	0
10^{3}	0	0	0	0	0	0	0	0
$10^{3.5}$	0	0	0	1	0	0	0	0
	NMS8RP				MS8RP			
10	0	1	0	0	0	1	0	0
$10^{1.5}$	0	1	0	0	0	0	0	0
10^{2}	0	0	0	1	0	0	0	0
$10^{2.5}$	0	0	0	1	0	0	0	1
10^{3}	0	0	0	2 (1)	0	1	0	0
$10^{3.5}$	0	0	0	5	0	0	0	1 (1)
	NMS8OP				MS8OP			
10	0	3	0	0	0	0	0	0
$10^{1.5}$	0	1	0	1	0	1	0	0
10^{2}	0	1	0	1 (1)	0	0	0	0
$10^{2.5}$	0	0	0	0	0	3	0	0
10^{3}	0	2	0	2	0	5	0	5 (1)
$10^{3.5}$	0	3	0	10 (4)	1	3	1	8 (6)

their $S_{\rm MAXI}$ can be missed as we use the tidal radius as a criterion for the ejection. Some ejected $S_{\rm MAXI}$ from massive clusters may not reach the clusters' tidal radius by 3 Myr due to their large tidal radius. Thus, the real ejection frequency would be higher than the above value for the massive clusters. By using $N_{\rm vesc10}$ (Table 3), the number of clusters whose $S_{\rm MAXI}$ has a velocity greater than the escape velocity of the cluster and has travelled beyond 10 pc from the cluster centre, the ejection frequency increases to 40 per cent for the cluster with $10^4\,M_\odot$ (circles in Fig. 4). In order to estimate the real probability for the $S_{\rm MAXI}$ ejection, in addition, we provide in Appendix A the number of clusters whose $S_{\rm MAXI}$ is found beyond the distance criterion using the half-mass radius for all models.

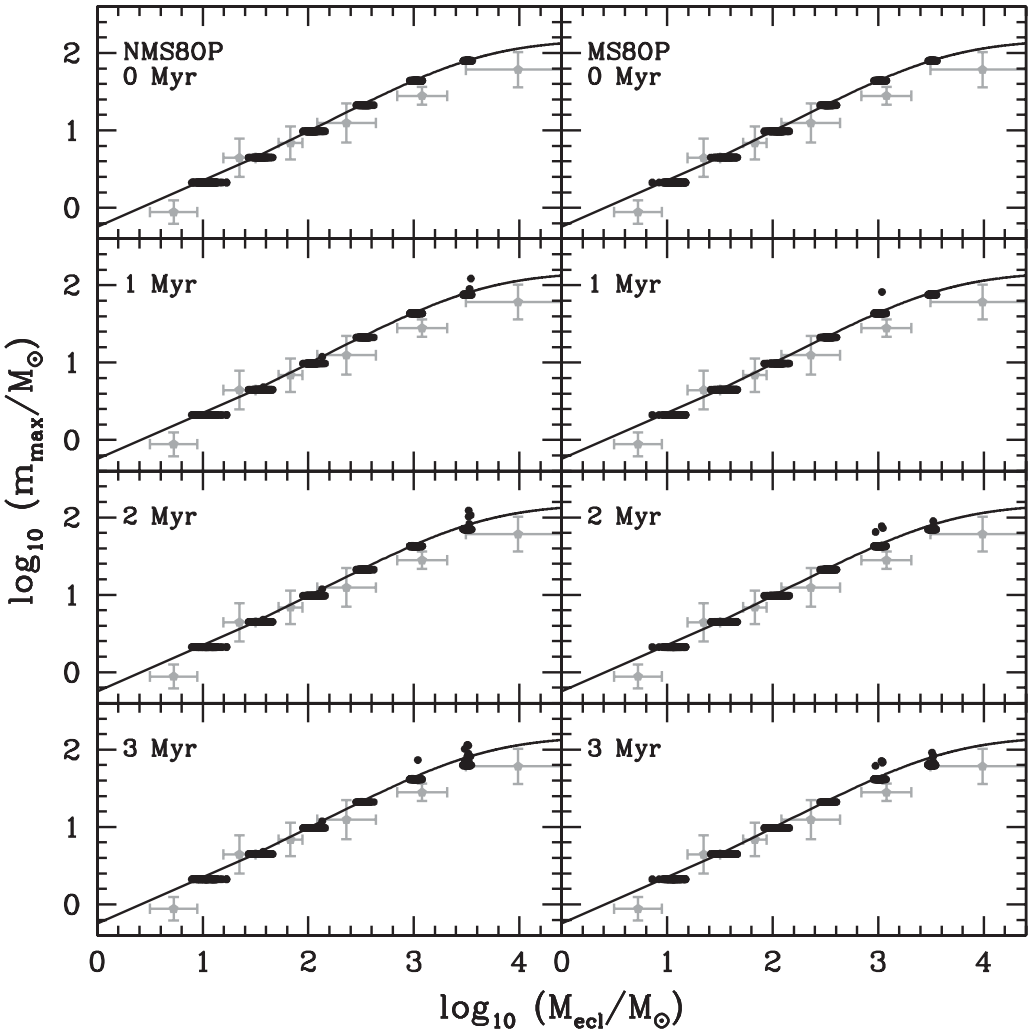

Figure 2. The mass of the most massive star versus the cluster mass for the unsegregated (left: NMS8OP) and the segregated (right: MS8OP) clusters with $r_{0.5} = 0.8$ pc and massive binaries with mass ratios biased towards unity at 0, 1, 2 and 3 Myr (from top to bottom). Each black point indicates a cluster. The grey data are the average observational data as in Fig. 1. The solid line represents the semi-analytical model from Weidner & Kroupa (2004, 2006) assuming an upper limit of stellar mass of 150 $M_\odot$ (equations 1 and 2). As we fix the number of stars at a certain cluster mass, the cluster mass slightly varies for each realization for the same cluster mass model. We only plot the result up to 3 Myr since the initially heaviest star of the cluster with $10^{3.5}$ $M_\odot$ loses a large amount of its initial mass within 3.5 Myr, thereafter stellar evolution affects the relation. The stars that appear above the solid curve are merger products.

From Figs 2 and 3 it is evident that collisions of massive stars may conceal the dynamical ejection of $S_{\rm MAXI}$ by the product of the collisions becoming more massive than the mass of the initially heaviest member. Thus, the dynamical behaviour of $S_{\rm MAXI}$ needs to be considered to distinguish whether it is ejected or not. Figs 5 and 6 show the distance from the cluster centre and the velocity of $S_{\rm MAXI}$ in NMS3OP and MS3OP clusters with 10 and $10^{3.5}$ $M_\odot$.

The heaviest stars are initially located at a wide range of radii up to ≈2.5 pc in the unsegregated cluster models (Fig. 5) while they are centrally concentrated in the segregated ones (Fig. 6). In both cases, massive stars sink towards the centre of the clusters due to dynamical friction and/or energy equipartition. This is more prominent in the unsegregated clusters since the heaviest stars already reside in the deep potential of the segregated clusters at the beginning of the calculations.

As shown in Figs 5 and 6, the heaviest stars hardly attain a high velocity if the massive stars are randomly paired into binaries. In RP, massive stars are mostly paired with low-mass stars; therefore, their mass ratios (m_2/m_1, where $m_1 \geq m_2$) are skewed to 0. Randomly paired massive binaries therefore behave like single stars. Clusters with massive binaries paired randomly do not shoot out their $S_{\rm MAXI}$ more frequently even though the clusters are initially mass segregated.

Clusters with massive binaries paired by OP and $M_{\rm ecl} \geq 100$ $M_\odot$ effectively produce heaviest stars with velocities exceeding the escape velocity of the cluster. For example, in the case of some initial conditions more than 20 per cent of the clusters show that their $S_{\rm MAXI}$ has a velocity larger than the escape velocity at 3 Myr (Table 3). It is known that massive stars are ejected from the small core of massive stars in the cluster centre lacking low-mass stars (Clarke & Pringle 1992). In the case of segregated clusters with OP massive binaries, the clusters already form with this kind of core; thus, the massive stars can be ejected at a very early age of the cluster (see Fig. 6). $S_{\rm MAXI}$ of one cluster with $M_{\rm ecl} = 10^{3.5}$ $M_\odot$ from the MS3OP model has travelled more than 200 pc from the cluster with a velocity of about 80 km s^{-1} at 3 Myr.

Although the low-mass clusters barely eject their $S_{\rm MAXI}$ regardless of their initial conditions, the binary-rich or binary-poor cases

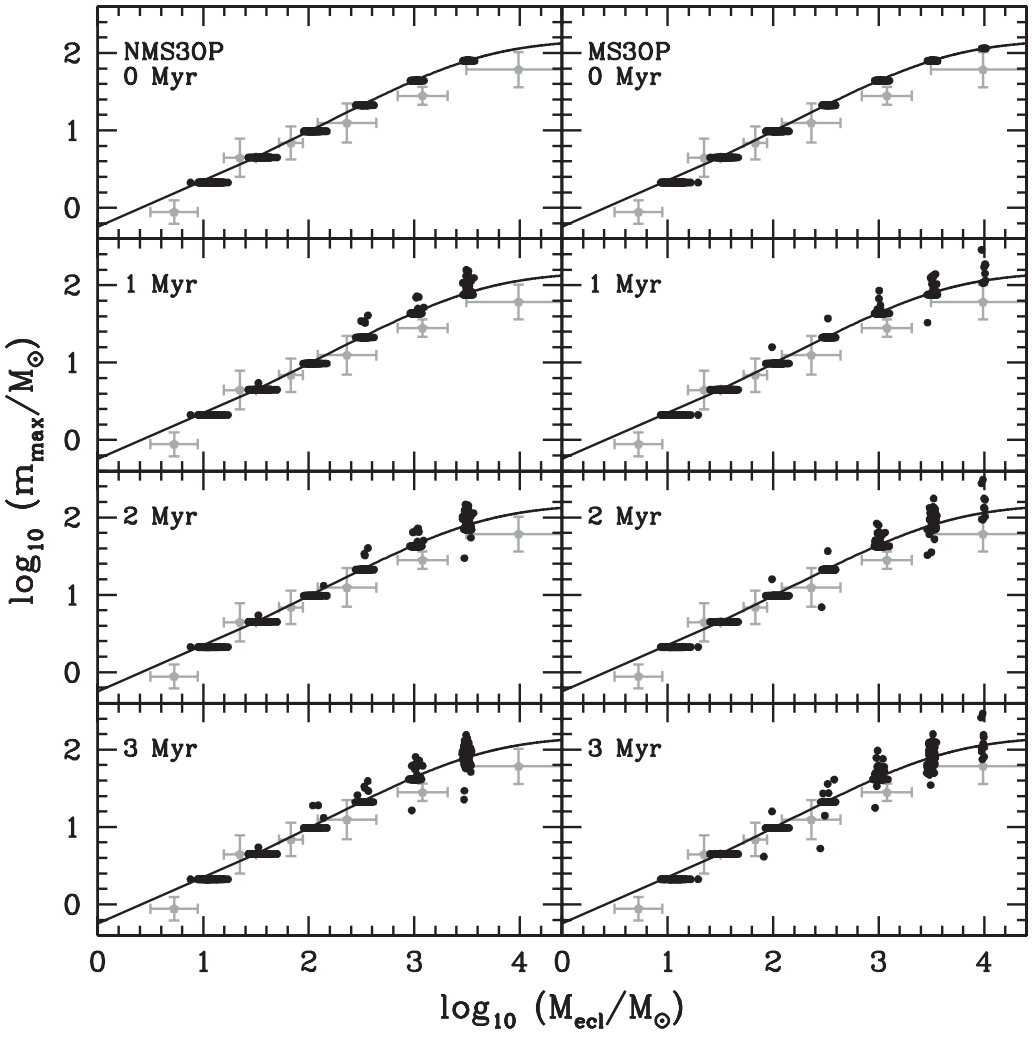

Figure 3. Same as Fig. 2, but for the OP clusters with $r_{0.5} = 0.3$ pc (left: NMS3OP; right: MS3OP).

show differences, e.g., the number of clusters whose $S_{\rm MAXI}$ has a velocity greater than the escape velocity is larger for binary-rich clusters. For massive clusters, on the contrary, binary-poor and binary-rich clusters with RP show similar results in the case of unsegregated models. Primordial mass segregation enhances the ejection of the most massive star at earlier times and helps more clusters shoot out their $S_{\rm MAXI}$ within 3 Myr.

3.2 Stellar collisions

$m_{\rm max}$ can increase by stellar collisions, either involving $S_{\rm MAXI}$ or not, which makes a star heavier than the mass of $S_{\rm MAXI}$ before the collisions occur. Although stellar collisions occur over a whole range of stellar masses, in this study, we only care about the collision that changes $m_{\rm max}$. The occurrences of the collisions are contained in Table 3.

For clusters with $r_{0.5} = 0.8$ pc [$2 < \rho_{0.5} < 750\,{\rm M}_\odot\,{\rm pc}^{-3}$, where $\rho_{0.5} = 3M_{\rm ecl}/(8\pi r_{0.5}^3)$ is the average mass density within the half-mass radius] stellar collisions rarely occur in them due to their low density. In single star cluster models (NMS8S and MS8S), only one cluster shows that its $m_{\rm max}$ changes by a stellar collision which involves $S_{\rm MAXI}$. In the case of binary-rich models there are a few clusters whose $m_{\rm max}$ changes via stellar collisions, mostly in the most massive cluster models, but with a probability of less than 10 per cent taking all models into account. In low-density ($r_{0.5} = 0.8$ pc) clusters a change of $m_{\rm max}$ through stellar collisions is highly improbable.

For clusters with $r_{0.5} = 0.3$ pc, the stellar collision result of low-mass clusters, $M_{\rm ecl} \leq 10^{2.5}\,{\rm M}_\odot$ ($\rho_{0.5} \lesssim 1400\,{\rm M}_\odot\,{\rm pc}^{-3}$), is similar to the result from clusters with $r_{0.5} = 0.8$ pc. But in the case of the massive cluster models ($M_{\rm ecl} \geq 10^3\,{\rm M}_\odot$), especially the most massive one, about half of them experience a change of $m_{\rm max}$ by stellar collisions.

Most of the collisions are induced by binary encounters, in which the two components of a binary system collide due to their highly eccentric orbit generated by perturbation through other stars. Direct dynamical collisions are extremely rare. This naturally explains why $N_{\rm c}$ in Table 3 becomes larger when clusters are initially binary rich. And the number increases when massive binaries are paired with the OP method when compared to RP. This can be understood because both components of a massive binary in the OP method are massive stars and thus have larger sizes leading to collisions. With a different collision channel from our result, Gaburov, Gualandris & Portegies Zwart (2008) also showed that a binary is more efficient in stellar collisions than a single star as the enhanced cross-section of a binary compared to a single star results in other stars engaging

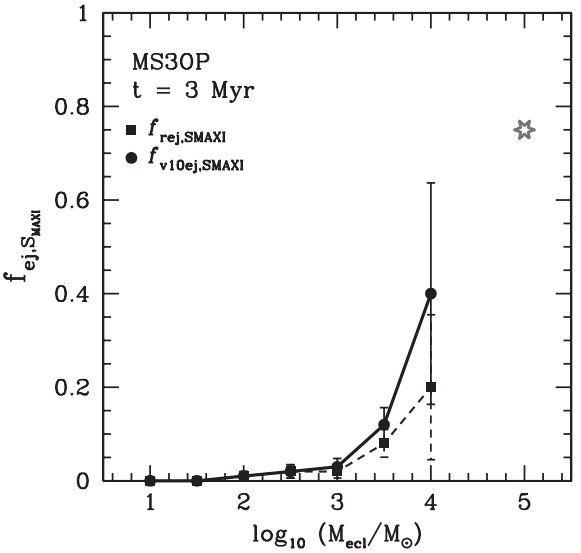

Figure 4. The ejection frequency of $S_{\rm MAXI}$ as a function of the cluster mass for mass-segregated clusters with massive binaries (MS3OP) at 3 Myr. $f_{\rm rej,S_{MAXI}}$, marked with squares, is the ratio of the number of clusters whose $S_{\rm MAXI}$ is located further than the tidal radius from the cluster centre, $N_{\rm resc}$ in Table 3, to the total number of the realizations, $N_{\rm run}$, which is 100 in our study for each initial condition set (10 for $10^4\,{\rm M}_\odot$ clusters). The error bars indicate Poisson uncertainties. All other models have $f_{\rm rej,S_{MAXI}} \approx 0$ (Table 3). The circles, $f_{\rm v10ej,S_{MAXI}}$, are the ratio of $N_{\rm vesc10}$ (Table 3) to $N_{\rm run}$. $f_{\rm v10ej,S_{MAXI}}$ is probably closer to the real ejection frequency as some massive clusters which eject their $S_{\rm MAXI}$ can be missed in $N_{\rm resc}$ due to their large tidal radii. The grey star is the ejection frequency of $S_{\rm MAXI}$ from clusters with $M_{\rm ecl} = 10^5\,{\rm M}_\odot$ taken from the calculations by Banerjee et al. (2012). These authors refer to a star that is ejected when its distance from the cluster centre is larger than 10 pc. Note that the initial conditions of their calculations are different but comparable to our MS3OP models.

the binary, and then this can lead to a collision between one of the binary components and the incoming third star.

Both the dynamical ejection of $S_{\rm MAXI}$ and stellar collisions that increase $m_{\rm max}$ barely take place in the same cluster within the cluster mass range we study. As shown by Baumgardt & Klessen (2011) and Moeckel & Clarke (2011), stellar collisions generally lead to the formation of a single very massive star through the merging of several massive stars rather than the formation of many massive stars. This single very massive star is hardly ejected from the cluster and its formation reduces the number of massive stars; thus, it may hamper the ejection of other massive stars. Out of 7200 cluster models (excluding the $10^4\,{\rm M}_\odot$ clusters from the MS3OP model), there are only three clusters in which both events occur. In one cluster $S_{\rm MAXI}$ is dynamically ejected, but one massive binary in the cluster merges then becoming more massive than $S_{\rm MAXI}$. In the other two clusters their $S_{\rm MAXI}$ gains mass by the collision with another star and then it is dynamically ejected.

Although this event is very rare, the most massive star in the star-forming region LH 95 in Large Magellanic Cloud (Da Rio et al. 2012) might be an example. The peculiarities of the star, with a much younger age than the average age of other stars in the region and the mass being higher than $m_{\rm max}$ from the Weidner & Kroupa (2004) $m_{\rm max}-M_{\rm ecl}$ relation, could have resulted from a stellar collision between binary components with similar masses of which the primary star may have been the initially most massive star of one of the three main substructures in the region, with a mass following the $m_{\rm max}-M_{\rm ecl}$ relation from Weidner & Kroupa (2004). The stellar collision could have increased the stellar mass and rejuvenated the star. And the ejection of the star with a low velocity can explain the location of the star which is at a rather far ($\approx$10 pc) distance from any of the substructures but still within the region.

3.3 The spread of $m_{\rm max}$

Fig. 7 presents the standard deviation of $\log m_{\rm max}$, $\sigma_{\rm lmmax}$, for the observed samples and our models. The observed larger $m_{\rm max}$ spread than what emerges from our models may be a result of stochastic effects of star formation as the dynamical processes hardly influence the change of $m_{\rm max}$ in these clusters, as shown by this study. However, numerical simulations of star cluster formation show that $m_{\rm max}$ and $M_{\rm ecl}$ evolve tightly following the relation $m_{\rm max} \propto M_{\rm ecl}^{2/3}$ (Bonnell et al. 2004; Peters et al. 2010).

For low-mass clusters ($M_{\rm ecl} < 100\,{\rm M}_\odot$) the differences between $\sigma_{\rm lmmax}$ of the observation and our model are large despite taking into account the spread due to the different cluster masses in the bins of observational data. This could be due to the large uncertainties of the observations. Note that the homogeneous data set from Kirk & Myers (2011) is more confined to the relation than the inhomogeneous data from Weidner et al. (2010) which come from many different references.

The spread in our models for relatively massive clusters ($M_{\rm ecl} \geq 10^3\,{\rm M}_\odot$) is comparable to the observed one in the case of clusters with $r_{0.5} = 0.3$ pc and with OP for massive binaries (NMS3OP and MS3OP models).

Stellar collisions dominate the change of $m_{\rm max}$ of relatively dense clusters with $M_{\rm ecl} \geq 10^{2.5}\,{\rm M}_\odot$ and $r_{0.5} = 0.3$ pc (Table 3) and therefore the spread of $m_{\rm max}$ of these clusters mostly comes from the collisions. However, it should be noted that the exact solution for the stellar collision process is as yet poorly understood. The treatment of stellar collisions in the code is simply adding the masses of two stars. Thus, the collision products shown in this study provide only a rough idea about merger rates and their masses. Therefore, we cannot quantify the real spread produced by the collisions but we expect that it would be smaller than our result since in reality not all the stellar mass ends up being in the merger product.

4 DISCUSSION

Fig. 8 shows the initial and the final ($t = 3$ Myr) mass functions of MS3OP model clusters. Massive stars are overpopulated in a cluster with a bump at the most massive stellar mass bin of the cluster's mass function because we enforce all clusters to have a star with a mass of $m_{\rm max,WK}$. As a necessary condition for massive star ejections is a small core of massive stars, the overpopulation of massive stars would enhance the ejection of massive stars. The other effect that might result from this choice is the overspread of $m_{\rm max}$ in low-mass (i.e. small-number) clusters if many of the clusters eject their $S_{\rm MAXI}$. When stellar masses are randomly drawn from the IMF low-mass clusters would hardly have a star with a mass close to $m_{\rm max}$ while massive clusters, that populate stars over the whole mass range, would have a few. However, the dynamical ejection of the most massive star from the low-mass cluster is highly improbable thus enforcing clusters to have a star with a $m_{\rm max,WK}$ would not have an impact on the spread.

The orbital parameters of the massive binaries are important for the ejection of massive stars. But our knowledge of their initial distribution functions is still poor. We use the same period distribution for massive binaries as that of low-mass stars. However,

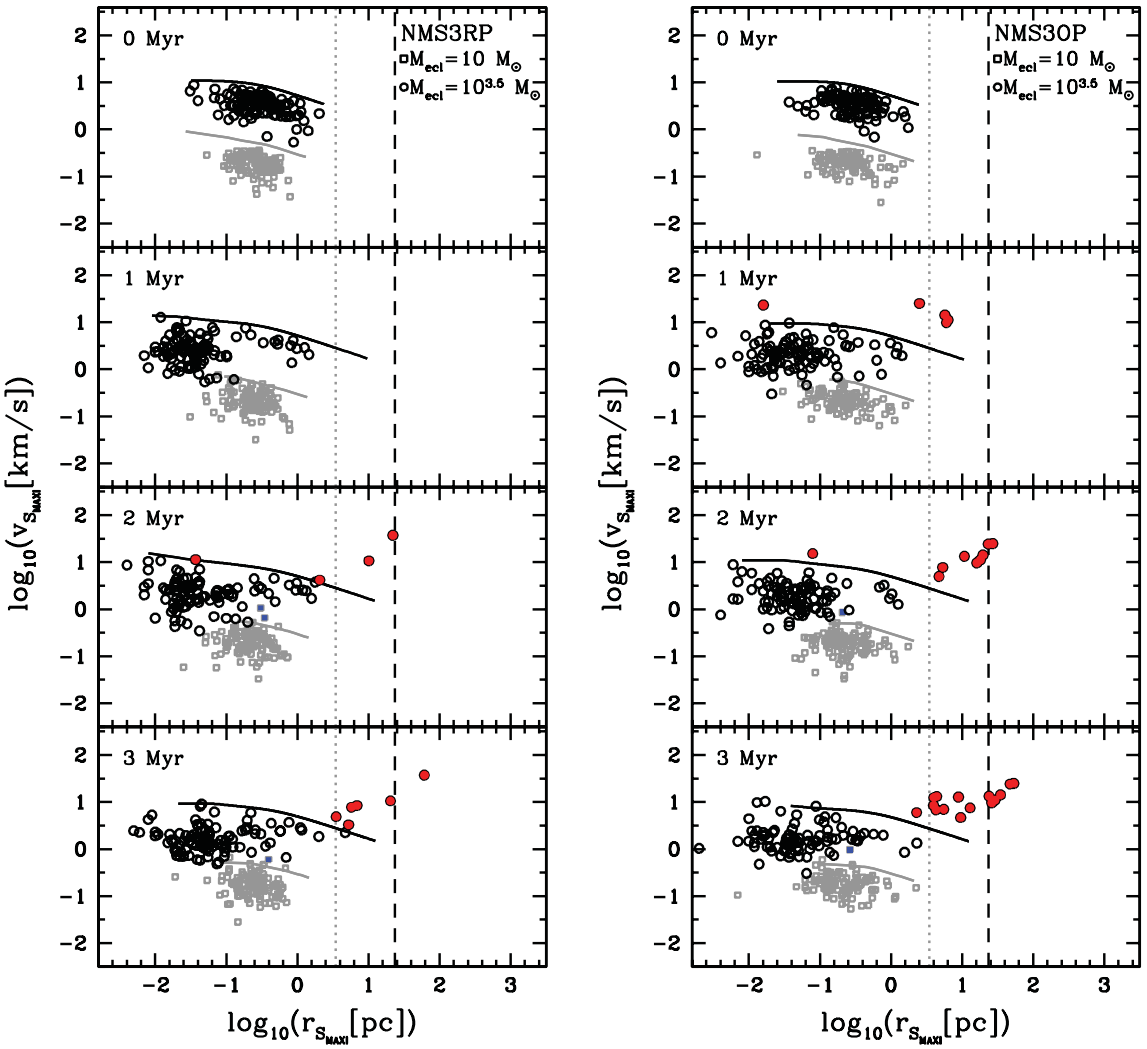

Figure 5. Distances from the cluster centre and velocities of $S_{\rm MAXI}$ stars of the initially unsegregated binary-rich clusters with $r_{0.5} = 0.3$ pc (left: NMS3RP; right: NMS3OP). Each dot denotes a cluster and in total there are 100 dots per configuration. The squares and circles are the values of $S_{\rm MAXI}$ in the clusters with 10 and $10^{3.5}$ $M_\odot$, respectively. The filled symbols represent $S_{\rm MAXI}$ stars with a speed exceeding the escape velocity. The black (grey) solid curves are the escape velocity of one cluster with $10^{3.5}$ (10) $M_\odot$ as a function of the distance from the cluster centre at each Myr. The grey dotted and the black dashed vertical lines indicate the initial tidal radius of the cluster with 10 and $10^{3.5}$ $M_\odot$, respectively. Note how mass segregation develops by 1 Myr and how OP increases the occurrence of ejected most massive stars.

a high fraction of short-period massive binaries are suggested by observations (Sana & Evans 2011) implying that massive binaries may have a different initial period distribution, compared to that of low-mass binaries. Dynamical ejections of the most massive star might become more likely than presented here. Future work taking into account the most recent constraints on the period distribution of massive star binaries will investigate this issue. The results for $M_{\rm ecl} \leq 10^3\,M_\odot$ clusters presented here will, however, not be affected as such clusters do not contain many, if any, massive stars.

Apart from our MS3OP sequence of models, our young star cluster library does not contain clusters more massive than $10^4\,M_\odot$ as they are computationally expensive due to the large binary population, while the observational sample contains a few clusters more massive than $10^4\,M_\odot$. At a higher density massive clusters may show the ejection of the heaviest star with a higher probability. Indeed, 20 per cent of the MS3OP clusters with $M_{\rm ecl} = 10^4\,M_\odot$ eject their $S_{\rm MAXI}$ (Fig. 4). Furthermore, three out of four clusters with $M_{\rm ecl} = 10^5\,M_\odot$ computed by Banerjee et al. (2012) eject their $S_{\rm MAXI}$. Further work including such massive clusters will be carried out to study this issue.

5 CONCLUSIONS

We have established a large theoretical young star cluster library using Aarseth's direct N-body integration code, NBODY6, with 73 different combinations of initial conditions such as cluster size and mass, initial binary population and primordial mass segregation. The library contains two different sizes of clusters, $r_{0.5} = 0.3$ and 0.8 pc, with two different binary fractions, zero and unity. In order to take into account that observed OB binaries likely have companions with similar masses, we generate clusters with massive binaries not only paired randomly from the IMF but also having a mass ratio close to unity. In both cases the stars follow the canonical IMF. And we model the initially mass-segregated clusters as well as unsegregated clusters. Using this library we study the $m_{\rm max}-M_{\rm ecl}$ relation

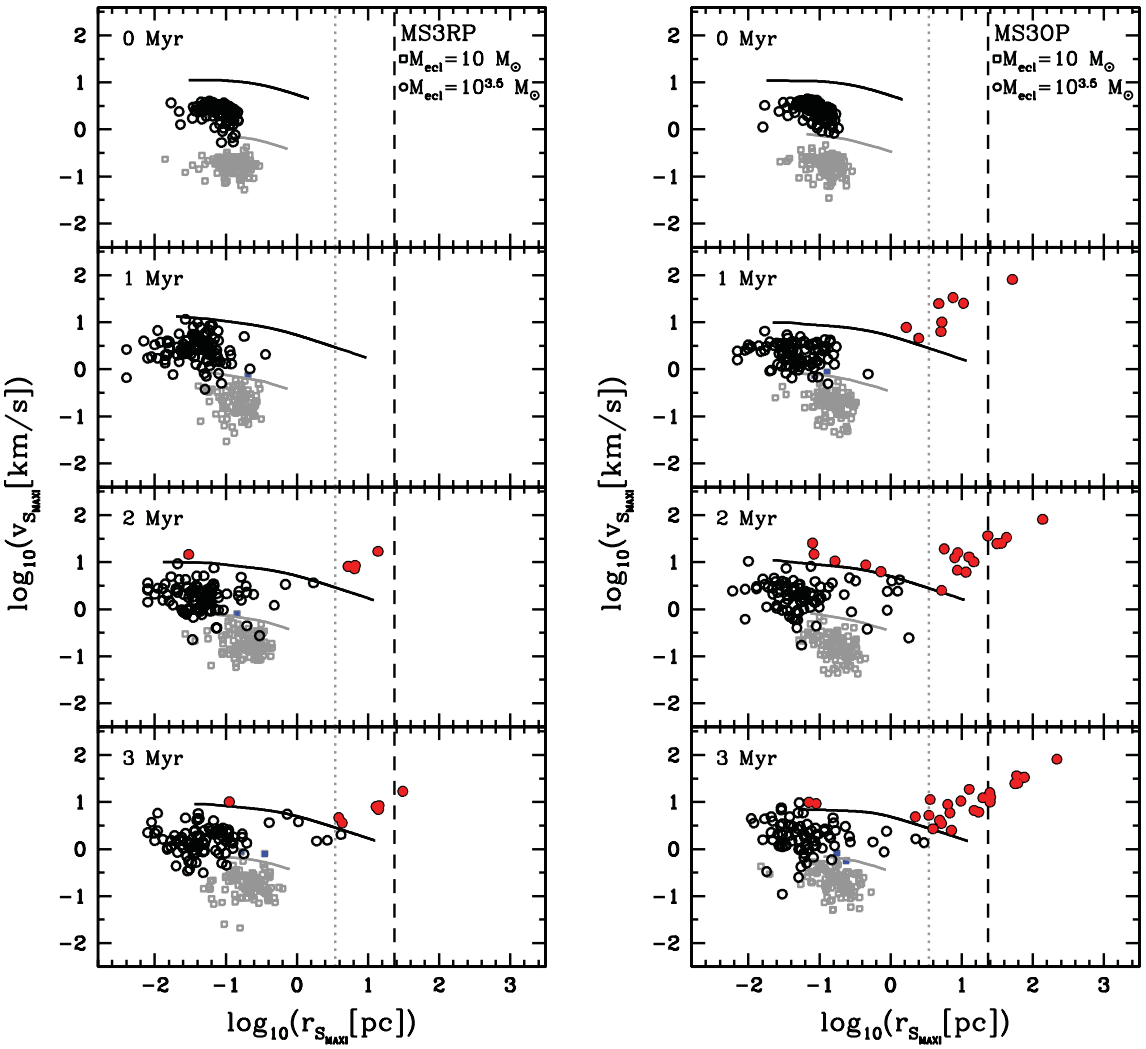

Figure 6. Same as Fig. 5 but for the initially mass-segregated, binary-rich clusters with $r_{0.5} = 0.3$ pc (left: MS3RP; right: MS3OP).

during the early evolution ($\leq$3 Myr) of the star clusters focusing on the effects on it established through dynamical ejection of the heaviest star from the cluster under the various initial conditions. Such computations of fully mass-segregated, binary-rich clusters have never been performed before.

Stellar evolution, stellar collision and dynamical ejection can alter the $m_{\rm max}$ of the cluster. In our models, all three effects are observed to affect $m_{\rm max}$. Stellar evolution affects the relation only for the massive ($\gtrsim 10^3$ M$_\odot$) clusters since only stars more massive than 40 M$_\odot$ significantly lose their mass within 3 Myr. Furthermore, since the mass of $S_{\rm MAXI}$ is the same for the same cluster mass, stellar evolution cannot contribute to the spread of $m_{\rm max}$ in this study. Stellar collisions influence mainly massive clusters, especially for those with the smaller radius as the clusters are denser. For clusters with $r_{0.5} = 0.3$ pc and $M_{\rm ecl} = 10^{3.5}$ M$_\odot$, for about half of the clusters their $m_{\rm max}$ has changed by stellar collisions within 3 Myr. Lastly, concerning the focus of this study, the dynamical ejection of $S_{\rm MAXI}$ only occurs in the binary-rich clusters with $r_{0.5} = 0.3$ pc and $M_{\rm ecl} > 10^2$ M$_\odot$. The number of the ejections increases when massive binaries are paired with the OP method and/or are initially concentrated in the cluster centre. As massive clusters likely have a few stars with masses close to the mass of $S_{\rm MAXI}$, $m_{\rm max}$ value would change little for massive clusters when $S_{\rm MAXI}$ is dynamically ejected. Overall we conclude that (dynamical) evolutionary effects hardly produce a spread of $m_{\rm max}$ in the relation for low-mass ($M_{\rm ecl} \lesssim 10^{2.5}$ M$_\odot$) or less dense ($r_{0.5} = 0.8$ pc) clusters. Massive ($M_{\rm ecl} = 10^{3.5}$ M$_\odot$), binary-rich clusters with $r_{0.5} = 0.3$ pc do show a significant spread of $m_{\rm max}$, mostly produced by stellar collisions, becoming comparable to the observed spread (Fig. 7).

Concerning the dynamical ejection of $S_{\rm MAXI}$, we find that in general it is very unlikely even in relatively dense clusters with massive binaries with similar mass companions. However, its probability can reach up to 20 per cent in our cluster library depending on the initial configuration of the cluster. For example, none of the clusters without initial mass segregation but with OP binaries and with $M_{\rm ecl} = 10^{3.5}$ M$_\odot$ and $r_{0.5} = 0.8$ pc (NMS8OP model) eject their $S_{\rm MAXI}$, while eight (two) out of 100 (10) mass-segregated clusters with $M_{\rm ecl} = 10^{3.5}(10^4)$ M$_\odot$ and $r_{0.5} = 0.3$ pc (MS3OP model) eject their $S_{\rm MAXI}$ (Table 3). In reality, many young star clusters are observed to fulfil the conditions which are needed to eject their massive star, such as having a compact size and massive binaries with similar component masses, so that some (up to $\approx$75 per cent for 10^5 M$_\odot$ clusters, see Fig. 4) of the real embedded clusters could have lost their initially most massive star by dynamical ejection within 3 Myr.

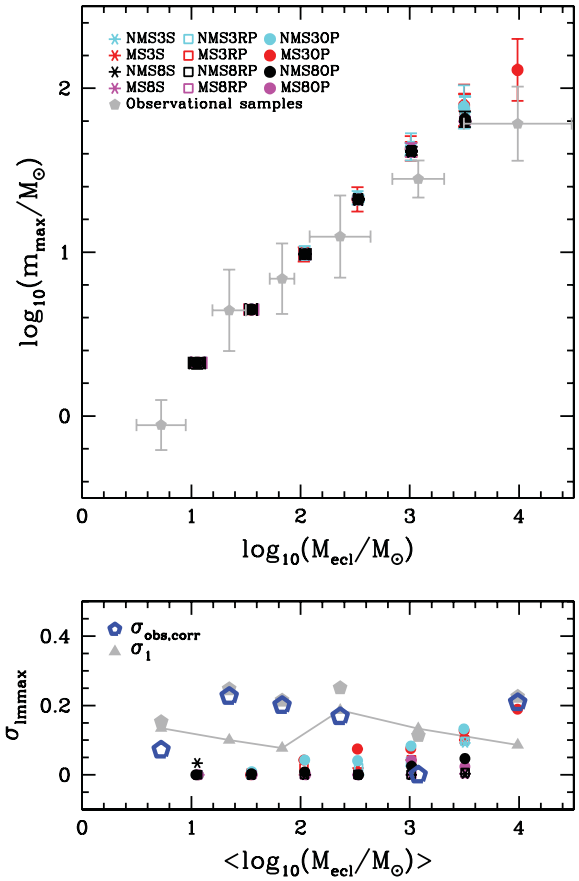

Figure 7. Top: average $m_{\rm max}-M_{\rm ecl}$ plot for all models at 3 Myr. The error bars indicate the standard deviations of $M_{\rm ecl}$ and $m_{\rm max}$. The grey symbols are the observed cluster samples as in Figs 2 and 3. The colour and symbol codes are given in the upper-left corner of the figure. Bottom: standard deviation of $\log_{10}m_{\rm max}$, $\sigma_{\rm lmmax}$, for each cluster model from the top figure. The colours and symbols are the same as in the top panel. Note that for $M_{\rm ecl} \leq 10^{2.5}\,{\rm M}_\odot$ the observed $\sigma_{\rm lmmax}$, $\sigma_{\rm obs}$, is much larger than the dispersion in the models. To quantify the deviation due to binning the cluster mass in the observed range of cluster masses in each mass bin, we obtain $m_{\rm max}$ according to equations (1) and (2) with $m^*_{\rm max} = 150\,{\rm M}_\odot$ for the observed cluster masses. We then calculate the standard deviation of $\log_{10}m_{\rm max}$, σ_1, by binning the clusters in the same way as for $\sigma_{\rm obs}$. This is shown as grey triangles connected with a solid line. The corrected observed $\sigma_{\rm lmmax}$, $\sigma_{\rm obs,corr} = \sqrt{\sigma^2_{\rm obs} - \sigma^2_1}$ (if $\sigma_{\rm obs} > \sigma_1$ otherwise $\sigma_{\rm obs,corr} = 0$), is plotted with blue open pentagons.

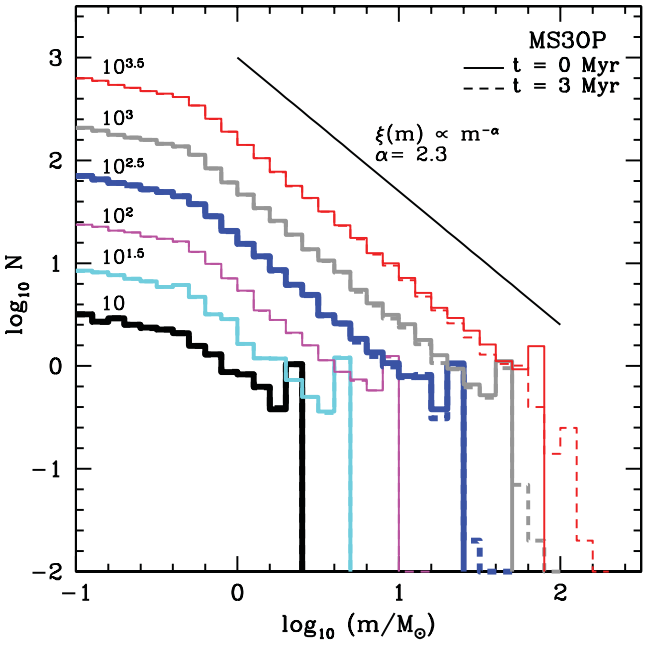

Figure 8. Mass functions of MS3OP clusters. Each line indicates the average mass function of clusters obtained from the 100 computations per model with a mass of 10, $10^{1.5}$, 10^2, $10^{2.5}$, 10^3 and $10^{3.5}\,{\rm M}_\odot$ from the bottom to the top. The solid and dashed histograms are mass functions at 0 (initial) and 3 Myr, respectively. A solid line on top of the histograms is the Salpeter mass function.

In this paper, we are only interested in the heaviest star of the cluster. However, the dynamical ejection of other massive stars in the cluster is also interesting because it is important to understand the origin of field massive stars and OB runaways (Fujii & Portegies Zwart 2011) to help us to constrain the initial configuration of massive stars in clusters. The dynamical ejections of OB stars in our theoretical young star cluster library will be discussed in the following paper (Oh et al. in preparation), and Banerjee et al. (2012) and Pflamm-Altenburg & Kroupa (2006) have, respectively, already demonstrated that R136-type starburst and ONC -type clusters are very efficient in ejecting OB stars.

ACKNOWLEDGMENTS

We are very grateful to Sverre Aarseth for making his NBODY6 freely available and continuing its improvements and to Vasilii Gvaramadze for useful comments. SO was supported for this research through a stipend from the International Max Planck Research School (IMPRS) for Astronomy and Astrophysics at the Universities of Bonn and Cologne as well as by a stipend from the Stellar Populations and Dynamics Research (SPODYR) Group at the AIfA and from the DAAD.

REFERENCES

Aarseth S. J., 1999, PASP, 111, 1333
Aarseth S. J., 2003, Gravitational N-Body Simulations. Cambridge Univ. Press, Cambridge
Aarseth S. J., Hénon M., Wielen R., 1974, A&A, 37, 183
Ahmad A., Cohen L., 1973, J. Comput. Phys., 12, 389
Banerjee S., Kroupa P., Oh S., 2012, ApJ, 746, 15
Bate M. R., 2009, MNRAS, 392, 590
Bate M. R., 2012, MNRAS, 419, 3115
Baumgardt H., Klessen R. S., 2011, MNRAS, 413, 1810
Baumgardt H., de Marchi G., Kroupa P., 2008, ApJ, 685, 247
Binney J., Tremaine S., 1987, Galactic Dynamics. Princeton Univ. Press, Princeton, NJ
Bonnell I., Vine S. G., Bate M. R., 2004, MNRAS, 349, 735
Chen L., de Grijs R., Zhao J. L., 2007, AJ, 134, 1368
Clarke C. J., Pringle J. E., 1992, MNRAS, 255, 423
Crowther P. A., Schnurr O., Hirschi R., Yusof N., Parker R. J., Goodwin S. P., Kassim H. A., 2010, MNRAS, 408, 731
Da Rio N., Gouliermis D. A., Rochau B., Pasquali A., Setiawan J., De Marchi G., 2012, MNRAS, 422, 3356
Figer D. F., 2005, Nat, 434, 192
Fujii M., Portegies Zwart S., 2011, Sci, 334, 1380
Gaburov E., Gualandris A., Portegies Zwart S., 2008, MNRAS, 384, 376
García B., Mermilliod J. C., 2001, A&A, 368, 122
Goodwin S. P., Kroupa P., 2005, A&A, 439, 565

Gouliermis D., Keller S. C., Kontizas M., Kontizas E., Bellas-Velidis I., 2004, A&A, 416, 137
Gvaramadze V. V., Bomans D. J., 2008, A&A, 490, 1071
Gvaramadze V. V., Gualandris A., 2011, MNRAS, 410, 304
Gvaramadze V. V., Gualandris A., Portegies Zwart S., 2009, MNRAS, 396, 570
Gvaramadze V. V., Kniazev A. Y., Kroupa P., Oh S., 2011, A&A, 535, A29
Heggie D., Hut P., 2003, The Gravitational Million-Body Problem: A Multidisciplinary Approach to Star Cluster Dynamics. Cambridge Univ. Press, Cambridge
Hills J. G., Fullerton L. W., 1980, AJ, 85, 1281
Hurley J. R., 2008, in Aarseth S. J., Tout C. A., Mardling R. A., eds, Lecture Notes in Physics, Vol. 760, Initial Conditions for Star Clusters. Springer-Verlag, Berlin, p. 283
Hurley J. R., Pols O. R., Tout C. A., 2000, MNRAS, 315, 543
Hurley J. R., Tout C. A., Pols O. R., 2002, MNRAS, 329, 897
Kirk H., Myers P. C., 2011, ApJ, 727, 64
Kouwenhoven M. B. N., Brown A. G. A., Goodwin S. P., Portegies Zwart S. F., Kaper L., 2009, A&A, 493, 979
Kroupa P., 1995a, MNRAS, 277, 1491
Kroupa P., 1995b, MNRAS, 277, 1507
Kroupa P., 2001, MNRAS, 322, 231
Kroupa P., 2002, Sci, 295, 82
Kroupa P., 2008, in Aarseth S. J., Tout C. A., Mardling R. A., eds, Lecture Notes in Physics Vol. 760, Initial Conditions for Star Clusters. Springer-Verlag, Berlin, p. 181
Kroupa P., Petr-Gotzens M. G., 2011, A&A, 529, A92
Kroupa P., Weidner C., Pflamm-Altenburg J., Thies I., Dabringhausen J., Marks M., Maschberger T., 2012, preprint (arXiv:1112.3340)
Leonard P. J. T., Duncan M. J., 1990, AJ, 99, 608
Marks M., Kroupa P., Oh S., 2011, MNRAS, 417, 1684
Maschberger T., Clarke C. J., 2008, MNRAS, 391, 711
Moeckel N., Clarke C. J., 2011, MNRAS, 410, 2799
Oey M. S., Clarke C. J., 2005, ApJ, 620, L43
Peters T., Klessen R. S., Mac Low M., Banerjee R., 2010, ApJ, 725, 134
Pflamm-Altenburg J., Kroupa P., 2006, MNRAS, 373, 295
Röser S., Schilbach E., Piskunov A. E., Kharchenko N. V., Scholz R.-D., 2011, A&A, 531, A92
Sana H., Evans C. J., 2011, in Neiner C., Wade G., Meynet G., Peters G., eds, Proc. IAU Symp. 272, Active OB Stars: Structure, Evolution, Mass Loss & Critical Limits. Cambridge Univ. Press, Cambridge, p. 474
Sana H., Gosset E., Nazé Y., Rauw G., Linder N., 2008, MNRAS, 386, 447
Sana H., Gosset E., Evans C. J., 2009, MNRAS, 400, 1479
Smith R. J., Longmore S., Bonnell I., 2009, MNRAS, 400, 1775
Thies I., Kroupa P., 2007, ApJ, 671, 767
Weidner C., Kroupa P., 2004, MNRAS, 348, 187
Weidner C., Kroupa P., 2006, MNRAS, 365, 1333
Weidner C., Kroupa P., Maschberger T., 2009, MNRAS, 393, 663
Weidner C., Kroupa P., Bonnell I. A., 2010, MNRAS, 401, 275

APPENDIX A: EJECTION ESTIMATES OF $S_{\rm MAXI}$ USING THE HALF-MASS RADIUS

The tidal radius is used in the paper to determine if a star belongs to the cluster. In some cases, even though $S_{\rm MAXI}$ is dynamically ejected through a strong close encounter the star may have not left the cluster yet at a given time, especially if it has obtained a relatively low velocity from the encounter. Thus, the real probability for ejection of $S_{\rm MAXI}$ may be higher than that presented in this paper. Considering that the massive stars are generally seated in the central part of the cluster due to dynamical interactions, relatively small distance such as the half-mass radius can be used as the ejection criterion for $S_{\rm MAXI}$. However, it should be noted that $S_{\rm MAXI}$ being found outside of the half-mass radius does not necessarily mean that it is ejected, especially when the cluster is initially unsegregated and dynamically unevolved. Here, therefore, we provide tables (Tables A1 and A2) which contain the mean half-mass radius and the number of clusters whose $S_{\rm MAXI}$ is found outside of $r_{0.5}$, $2r_{0.5}$ and $4r_{0.5}$ and additionally has a velocity greater than the escape velocity at the given time. For most of the cluster models the mean half-mass radii do not change much within 3 Myr due to the clusters' dynamical evolution. Note that the initial crossing time of the clusters with $M_{\rm ecl} \leq 100\,{\rm M}_{\odot}$ and $r_{0.5} = 0.8\,{\rm pc}$ is longer than 3 Myr (Table 2). The most expanded half-mass radius is $\approx$1 pc at 3 Myr, although a few massive cluster models have expanded up to twice their initial half-mass radius.

The initial positions of $S_{\rm MAXI}$ distinctly show whether the models are generated with initial mass segregation. For the initially unsegregated clusters (Table A1), more than half of the realizations for each models show that $S_{\rm MAXI}$ is initially located outside of the half-mass radius. Even in up to 23 (8) per cent of the clusters the star is located further out than $2r_{0.5}$ ($4r_{0.5}$) at 0 Myr. For the initially mass-segregated clusters, only in few low-mass clusters (less than 5 per cent at most) is $S_{\rm MAXI}$ located outside of $r_{0.5}$ at 0 Myr (Table A2). It may be strange for the mass-segregated cluster to show its most massive star having an initial position beyond the half-mass radius at all. But for the initially mass-segregated clusters with low masses ($M_{\rm ecl} < 100\,{\rm M}_{\odot}$) the initial position of $S_{\rm MAXI}$ can, sometimes, be generated slightly beyond the half-mass radius due to the shallow gravitational potential, the low number statistics and the algorithm generating the initially mass-segregated cluster (the heaviest star being the *most bound* to the cluster, but not requiring it to be at the most central position). None of the initially mass-segregated clusters have $S_{\rm MAXI}$ located initially further out than $2r_{0.5}$.

For the initially not mass-segregated clusters with relatively high masses ($\geq$100 $\,{\rm M}_{\odot}$) and/or $r_{0.5} = 0.3\,{\rm pc}$, $N(r_{S_{\rm MAXI}} > r_{0.5})$ in Table A1 significantly decreases at 3 Myr as a result of dynamical evolution, i.e. dynamical mass segregation. But there are still a large number of the unsegregated clusters, particularly the low-density ones, which have $S_{\rm MAXI}$ beyond the half-mass radius. In many cases the star has a velocity lower than the escape velocity. As those clusters are dynamically young and the velocity of the star is too small to escape from its cluster, it is unlikely that these stars are dynamically ejected. Either the star was initially located beyond the half-mass radius and has not fallen into the cluster centre yet. Or, if $S_{\rm MAXI}$ of the low-density clusters has an initial orbit as large as the half-mass radius (note that the half-mass radius is less than a parsec), it could be temporarily found beyond the half-mass radius since the dynamical interactions which lead to the massive star being confined to the central part of the cluster are insufficient by 3 Myr for these low-density clusters. This can also explain that for the mass-segregated clusters with low masses, especially with $10\,{\rm M}_{\odot}$, $N(r_{S_{\rm MAXI}} > r_{0.5})$ increases at 3 Myr and most of these clusters have $S_{\rm MAXI}$ moving slower than the escape velocity. There are only two initially mass-segregated clusters with $10\,{\rm M}_{\odot}$ whose $S_{\rm MAXI}$ is found beyond twice the half-mass radius at 3 Myr. These are due to low-energy encounters expelling the stars from the core without ejecting them from the cluster. However, in the NMS3OP and MS3OP models and in massive ($\geq 10^3\,{\rm M}_{\odot}$) clusters from the other models, a number of clusters have $S_{\rm MAXI}$ being beyond the half-mass radius with a velocity larger than the escape velocity, which implies that the $S_{\rm MAXI}$ stars are dynamically ejected. The probability of $S_{\rm MAXI}$ ejection increases with cluster mass. 40 per cent of the $10^4\,{\rm M}_{\odot}$ MS3OP clusters have probably ejected their $S_{\rm MAXI}$.

Table A1. The averaged half-mass radius, $\langle r_{0.5}\rangle$, and the number of clusters whose $S_{\rm MAXI}$ is found beyond the half-mass radius, $N(r_{S_{\rm MAXI}} > r_{0.5})$, beyond $2r_{0.5}$, $N(r_{S_{\rm MAXI}} > 2r_{0.5})$ and beyond $4r_{0.5}$, $N(r_{S_{\rm MAXI}} > 4r_{0.5})$ at 0 and 3 Myr from the initially unsegregated clusters. The latter numbers at 3 Myr marked with † are the number of clusters whose $S_{\rm MAXI}$ fulfils the distance criteria and moves faster than the escape velocity ($v_{S_{\rm MAXI}} > v_{\rm esc}$).

$M_{\rm ecl}$ ($M_\odot$)	$\langle r_{0.5}\rangle$ (pc)		$N(r_{S_{\rm MAXI}} > r_{0.5})$			$N(r_{S_{\rm MAXI}} > 2r_{0.5})$			$N(r_{S_{\rm MAXI}} > 4r_{0.5})$		
	0 Myr	3 Myr	0 Myr	3 Myr	3 Myr†	0 Myr	3 Myr	3 Myr†	0 Myr	3 Myr	3 Myr†
NMS3S											
10	0.27	0.27	49	31	0	14	6	0	2	1	0
$10^{1.5}$	0.29	0.30	47	6	0	9	3	0	2	0	0
10^{2}	0.30	0.36	52	11	0	21	8	0	3	4	0
$10^{2.5}$	0.30	0.41	54	6	0	16	3	0	3	0	0
10^{3}	0.30	0.50	45	2	0	15	2	0	7	1	0
$10^{3.5}$	0.30	0.55	48	10	6	18	8	6	3	5	4
NMS3RP											
10	0.25	0.31	53	23	1	6	0	0	0	0	0
$10^{1.5}$	0.28	0.31	46	12	0	9	3	0	1	1	0
10^{2}	0.29	0.37	53	17	0	21	10	0	4	3	0
$10^{2.5}$	0.30	0.47	54	12	0	19	1	0	3	0	0
10^{3}	0.30	0.54	47	6	2	17	3	1	7	1	0
$10^{3.5}$	0.30	0.55	50	13	6	18	9	6	3	7	6
NMS3OP											
10	0.26	0.30	46	23	0	12	6	0	1	1	0
$10^{1.5}$	0.28	0.31	44	18	0	12	4	0	0	1	0
10^{2}	0.29	0.38	47	9	2	18	4	1	1	0	0
$10^{2.5}$	0.30	0.56	44	14	7	19	8	3	5	3	2
10^{3}	0.30	0.68	44	15	11	16	9	9	6	7	7
$10^{3.5}$	0.30	0.65	48	17	15	15	16	15	3	14	14
NMS8S											
10	0.70	0.67	45	39	0	11	10	0	4	4	0
$10^{1.5}$	0.79	0.77	58	50	0	17	19	0	3	3	0
10^{2}	0.79	0.81	49	35	0	10	9	0	1	1	0
$10^{2.5}$	0.80	0.82	49	25	0	22	16	0	8	8	0
10^{3}	0.80	0.84	43	18	0	16	5	0	4	3	0
$10^{3.5}$	0.81	0.86	38	10	0	16	3	0	3	1	0
NMS8RP											
10	0.68	0.67	51	46	0	12	12	0	0	1	0
$10^{1.5}$	0.74	0.75	46	46	0	18	16	0	3	3	0
10^{2}	0.79	0.82	43	34	0	15	13	0	1	1	0
$10^{2.5}$	0.80	0.82	51	20	0	16	13	0	2	1	0
10^{3}	0.80	0.84	41	13	0	14	9	0	4	4	0
$10^{3.5}$	0.80	0.85	52	18	0	15	7	0	5	2	0
NMS8OP											
10	0.69	0.68	39	42	0	8	11	0	0	0	0
$10^{1.5}$	0.76	0.76	48	34	0	10	10	0	1	2	0
10^{2}	0.77	0.81	45	20	0	10	7	0	2	2	0
$10^{2.5}$	0.79	0.85	63	32	0	23	13	0	6	6	0
10^{3}	0.81	0.88	53	18	2	18	8	2	2	4	1
$10^{3.5}$	0.80	0.93	44	12	1	17	3	0	0	2	0

Table A2. Same as Table A1 but for the initially mass-segregated cluster models. Note that only 10 realizations are performed for 10^4 $M_\odot$ clusters due to the expensive computing cost.

$M_{\rm ecl}$ ($M_\odot$)	$\langle r_{0.5}\rangle$ (pc)		$N(r_{S_{\rm MAXI}} > r_{0.5})$			$N(r_{S_{\rm MAXI}} > 2r_{0.5})$			$N(r_{S_{\rm MAXI}} > 4r_{0.5})$		
	0 Myr	3 Myr	0 Myr	3 Myr	3 Myr†	0 Myr	3 Myr	3 Myr†	0 Myr	3 Myr	3 Myr†
MS3S											
10	0.24	0.25	0	10	0	0	0	0	0	0	0
$10^{1.5}$	0.28	0.31	0	0	0	0	0	0	0	0	0
10^2	0.32	0.35	0	0	0	0	0	0	0	0	0
$10^{2.5}$	0.31	0.44	0	2	1	0	0	0	0	0	0
10^3	0.31	0.55	0	2	1	0	2	1	0	1	1
$10^{3.5}$	0.31	0.59	0	7	5	0	5	4	0	4	4
MS3RP											
10	0.23	0.29	4	25	1	0	2	0	0	0	0
$10^{1.5}$	0.29	0.30	3	2	0	0	0	0	0	0	0
10^2	0.30	0.39	0	3	0	0	0	0	0	0	0
$10^{2.5}$	0.31	0.47	0	3	3	0	1	1	0	1	1
10^3	0.31	0.57	0	3	3	0	3	3	0	2	2
$10^{3.5}$	0.31	0.59	0	11	6	0	9	6	0	8	6
MS3OP											
10	0.23	0.26	2	11	0	0	0	0	0	0	0
$10^{1.5}$	0.28	0.33	0	3	1	0	1	1	0	0	0
10^2	0.29	0.42	0	4	4	0	4	4	0	2	2
$10^{2.5}$	0.30	0.60	0	19	16	0	12	12	0	3	3
10^3	0.31	0.72	0	20	13	0	15	11	0	11	8
$10^{3.5}$	0.31	0.70	0	26	22	0	24	22	0	19	19
10^4	0.31	0.50	0	4	4	0	4	4	0	4	4
MS8S											
10	0.63	0.59	0	6	0	0	0	0	0	0	0
$10^{1.5}$	0.77	0.74	1	5	0	0	0	0	0	0	0
10^2	0.87	0.82	0	1	0	0	0	0	0	0	0
$10^{2.5}$	0.81	0.86	0	0	0	0	0	0	0	0	0
10^3	0.82	0.90	0	0	0	0	0	0	0	0	0
$10^{3.5}$	0.83	0.93	0	0	0	0	0	0	0	0	0
MS8RP											
10	0.60	0.57	3	3	0	0	0	0	0	0	0
$10^{1.5}$	0.74	0.70	0	8	0	0	0	0	0	0	0
10^2	0.81	0.82	0	3	0	0	0	0	0	0	0
$10^{2.5}$	0.82	0.85	0	2	0	0	0	0	0	0	0
10^3	0.83	0.90	0	0	0	0	0	0	0	0	0
$10^{3.5}$	0.83	0.95	0	0	0	0	0	0	0	0	0
MS8OP											
10	0.61	0.55	0	3	0	0	0	0	0	0	0
$10^{1.5}$	0.75	0.67	0	4	0	0	0	0	0	0	0
10^2	0.78	0.80	0	2	0	0	0	0	0	0	0
$10^{2.5}$	0.80	0.93	0	3	2	0	0	0	0	0	0
10^3	0.83	1.02	0	7	4	0	2	2	0	0	0
$10^{3.5}$	0.83	1.05	0	5	3	0	3	2	0	2	2

This paper has been typeset from a TEX/LATEX file prepared by the author.